# Comparison between the Results of Computational Fluid Dynamics Analysis and an Experiment Using Particle Image Velocimetry

Shunsuke Saka[1], Koji Sakai[1], Hiroki Ono[2]
[1]Meiji University, Tokyo, Japan
[2]Central Research Institute of Electric Power Industry, Tokyo, Japan

## Abstract

An experimental database for computational fluid dynamics (CFD) code validation is indispensable. However, the example made by the low-turbulence natural convection field becomes dominant where the subject is little. Therefore, an experimental study was conducted by using particle image velocimetry (PIV) in a model of a floor-heating room. Furthermore, the results of CFD analysis were compared with the experimental data.

Wind-velocity measurement using PIV was conducted for grasping the natural convective field in a floor-heating room model and expansion of the wind-velocity database for CFD-code validation. It was confirmed that PIV was mostly able to obtain the air-current properties of the natural convective field in the floor neighborhood.

## Introduction

It has become practical to use computational fluid dynamics (CFD) in recent years to advance interior thermal environment analysis, as this method is inexpensive and highly flexible. However, low-turbulence flows such as those in an electric floor-heating room exhibit low predictability. Further, a database of experimental measurements is indispensable for predictability inspection and analysis of the accuracy of CFD. However, there are few examples which handled low-turbulent natural convection field. Thus, the subject of this research is to confirm the predictive ability of CFD analysis for the case of an electric floor-heating room. A model of such a room was constructed and fluid-flow data were accumulated. The results were compared with those of PIV analysis to inspect the accuracy of CFD.

The distribution of temperature and the wind velocity have been measured by previous studies in a natural convective field. Although problems with performing measurements at the corners of intersections and the inner boundary layers, as well as problems of the efficiency of measuring conventional wind velocity, remain. The PIV methods developed in recent years are non-contact and can be used to measure the flow rate in the two-dimensional aspect. Moreover, it is possible to calculate velocity with a large number of measurement points by image processing in visualized measurement space. PIV can measure the neighborhoods at the corners

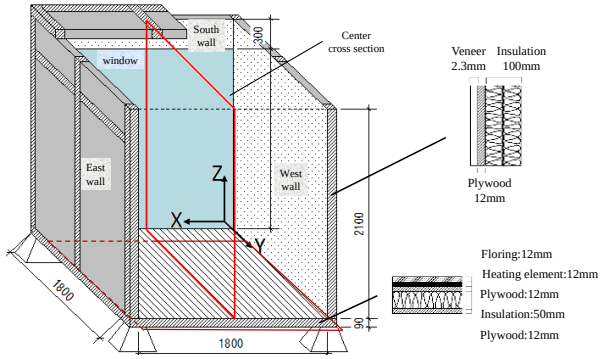


*Figure 1: A floor-heating room model.*

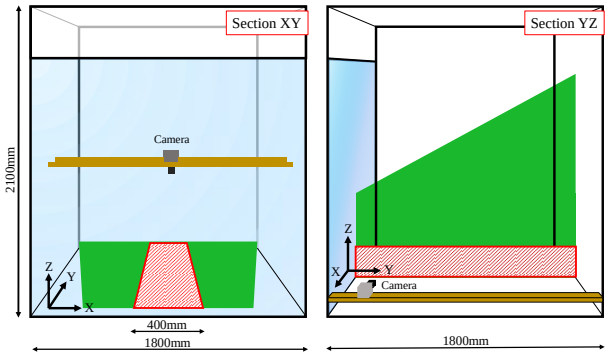


*Figure 2: Shooting method.*

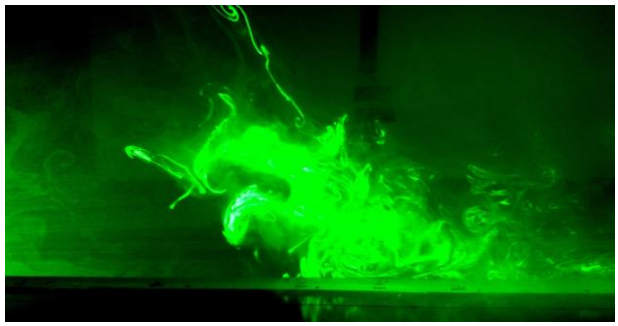

*Figure 3: Shooting by PIV.*

*Table 1: Measurement instruments*

| | |
|---|---|
| Tracer | PORTA SMOKE PS-2005 Dainichi Co. |
| Laser | PIV Laser G-450: 450 [mV] Kato-Koken Co. |
| Camera | Digital High Speed Camera HAS-L2 DITECT |
| Soft Ware | HAS- L2Basic for DPX-CLF400 DITECT |
| | Flownizer 2D(Ver.1.2.10.0) DITECT |

of intersections and resting faces in the room. It was difficult by a conventional anemometer. However, clear pictures and consideration of the setting during analysis are necessary to obtain highly precise measurements.

We performed visualization measurements of a natural convective field analyzed natural convection using PIV and CFD in a large enclosed cavity. It was consequently confirmed that comparison between PIV and CFD is useful. Further, the use of an advanced particle and a grasp of buoyancy and inertial force will be required henceforth. Thus, a wind-velocity measurement experiment in an actual large electric floor-heating room was performed. Moreover, its results were analyzed for the purpose of parametric study of PIV and expansion of actual measurement data.

## Experimental facility and procedure

### Experimental setup

The dimensions of the floor-heating-room model in a thermostatic room were 1,800 mm × 1,800 mm × 2,100 mm, yielding a two-dimensional flow, as shown in fig. 1. This study assumed the conditions of a winter night in Tokyo and set the external temperature to 5°C using air-conditioning equipment installed on the ceiling of the thermostatic room. When being regular, the surface around the resting face, the central of the room and the surface of the window side were isothermal at 30, 20, and 10°C, respectively.

A laser seat was irradiated perpendicular to the window side and the resting face during the experiment. And movie videos of the floor-surface neighborhood were taken. The analytical area was divided into 10 segments based on photographic restrictions. A target territory was shot for analysis 6 times and a mean velocity vector was calculated every 10 mm. The results of each of the 6 trials were averaged to improve the precision of the analysis by excluding bad data. The data from the case where smoke was unclear and the correlation coefficient was extremely low.

### Wind-velocity measurement by PIV

PIV was used to calculate wind-velocity vectors from fluctuations of the concentration distribution of a picture over 2 trials, as shown in fig. 3. The wind velocity was calculated by checking the smoke-concentration distribution in the interrogation region and determining the area where the correlation coefficient was highest in the search region of the next frame. Wind velocity vector in the instant when setting up a measurement point every 10mm and moving 1 frame as shown in fig. 4.

The relationship between the fluctuation of velocity and the correlation coefficient in randomly chosen coordinates is shown in fig. 5. When the correlation coefficient fell from these charts, the tendency of a large deviation to be generated in the velocity was confirmed. Therefore, the correlation coefficient was related to the reliability of the collected data, and a thing dependent on

*Table 2: PIV parameters*

| | | |
|---|---|---|
| Analysis algorithm | Direct-correlation PIV | |
| Spatial resolution | Section XY | 0.56[mm/pixel] |
| | Section YZ | 0.22[mm/pixel] |
| Interrogation Region | 48 × 48 pixels(10 mm × 10 mm) | |
| Photographing interval | 300[frame/sec] | |
| Full shooting time | 105 [sec] | |

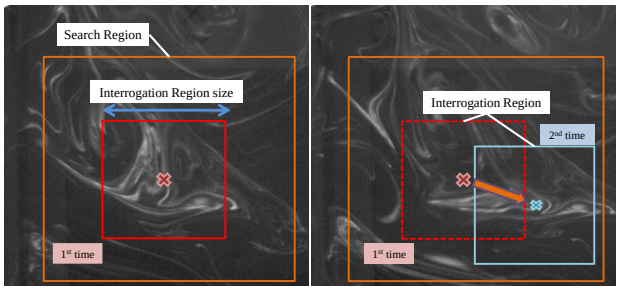


*Figure 4: Structures obtained by PIV.*

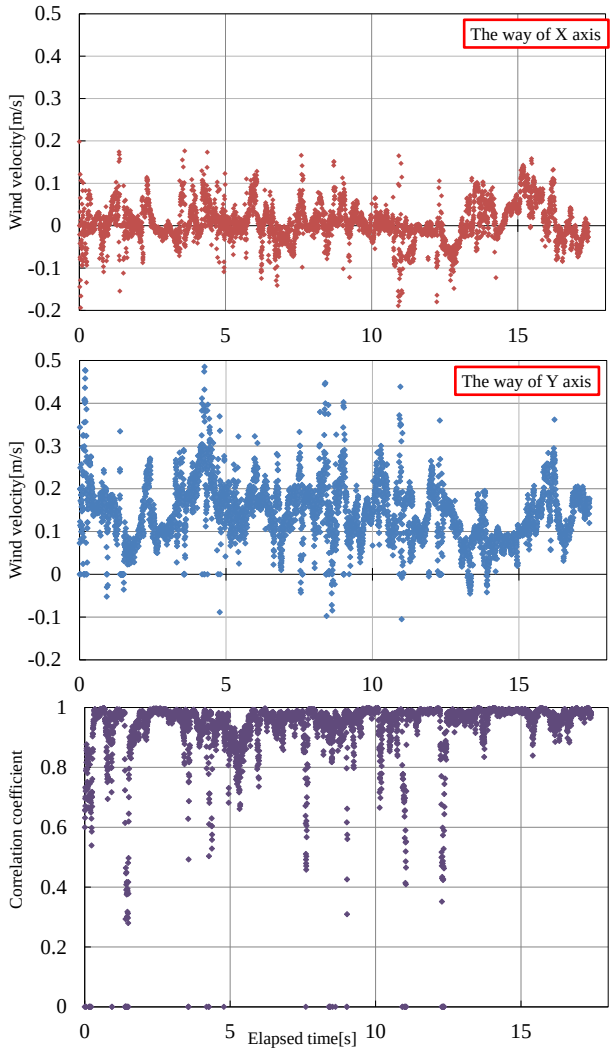


*Figure 5: Relationship between decrease in the correlation coefficient and the wind velocity.*

the setting of the search-region size was suggested. To perform a more precise inspection, there are some ways. Firstly, measuring long to reduce the influence of velocity components with particularly large deviations.

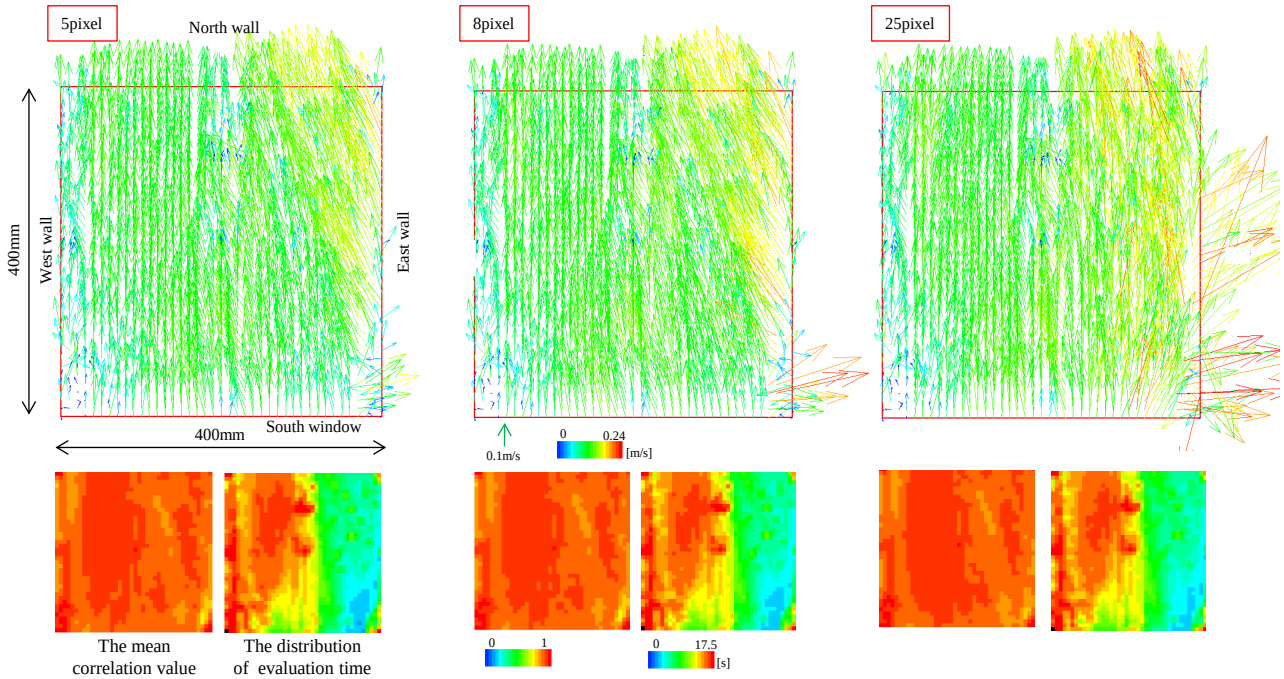


*Figure 6: A result of the inspection of the search-region size.*

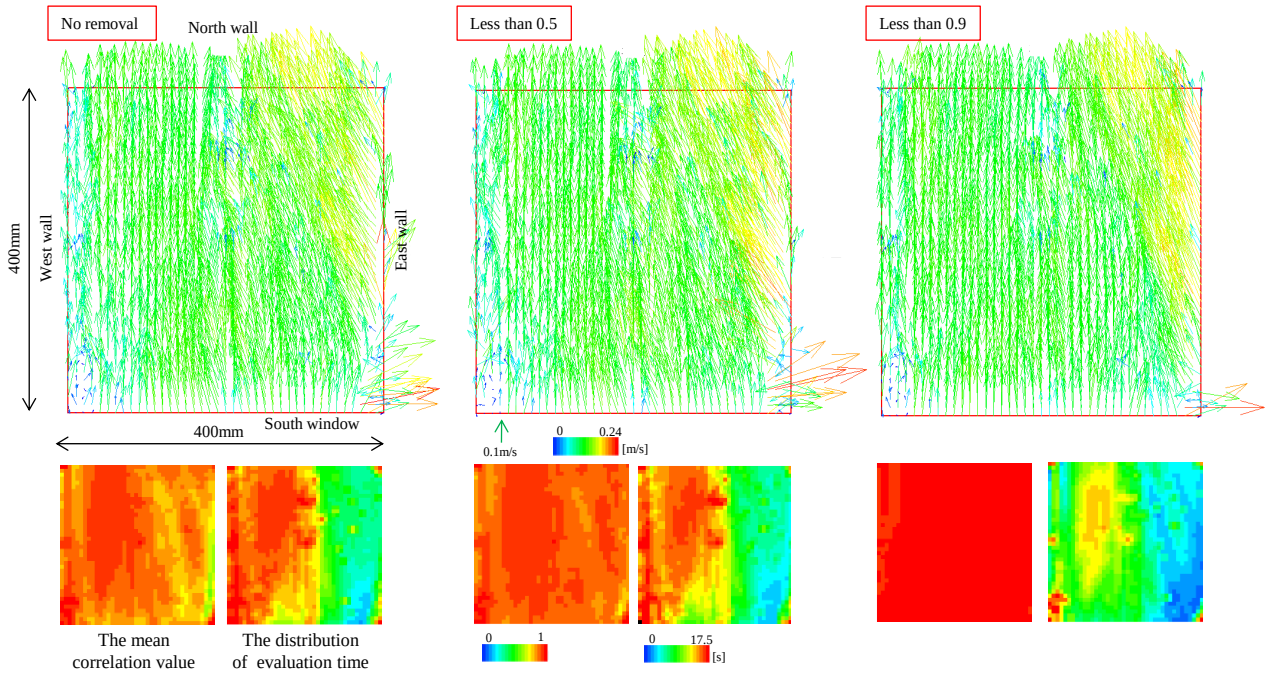


*Figure 7: A result of the inspection of error-vector removal.*

Secondly, a way to erase velocity component which the numerical value of the correlation coefficient below a certain, and it's necessary to decide like trial and error.

## Verification experiment

### Search-region size

The search-region size determines the maximum momentary wind velocity that can be observed. However, increasing the search-region size leads to the thing that calculates the low-correlation-coefficient wind velocity and a decline of the analytical efficiency. Therefore, the influence exerted by the search-region size upon the analytical result was inspected.

The mean wind-velocity vector and correlation value under changes of the search-region size are shown in fig. 6. The mean correlation value used in this figure is based on equalizing the correlation coefficients of each point respectively. Further, the evaluation-time distribution indicates the time of the data used for analysis of the animation. To compare regions with clearly identifiable smoke behavior with unclear regions, such characteristic animation was selected intentionally and the evaluation time on the left side of the region was long.

There were no significant changes in the average correlation value and the evaluation-time distribution as

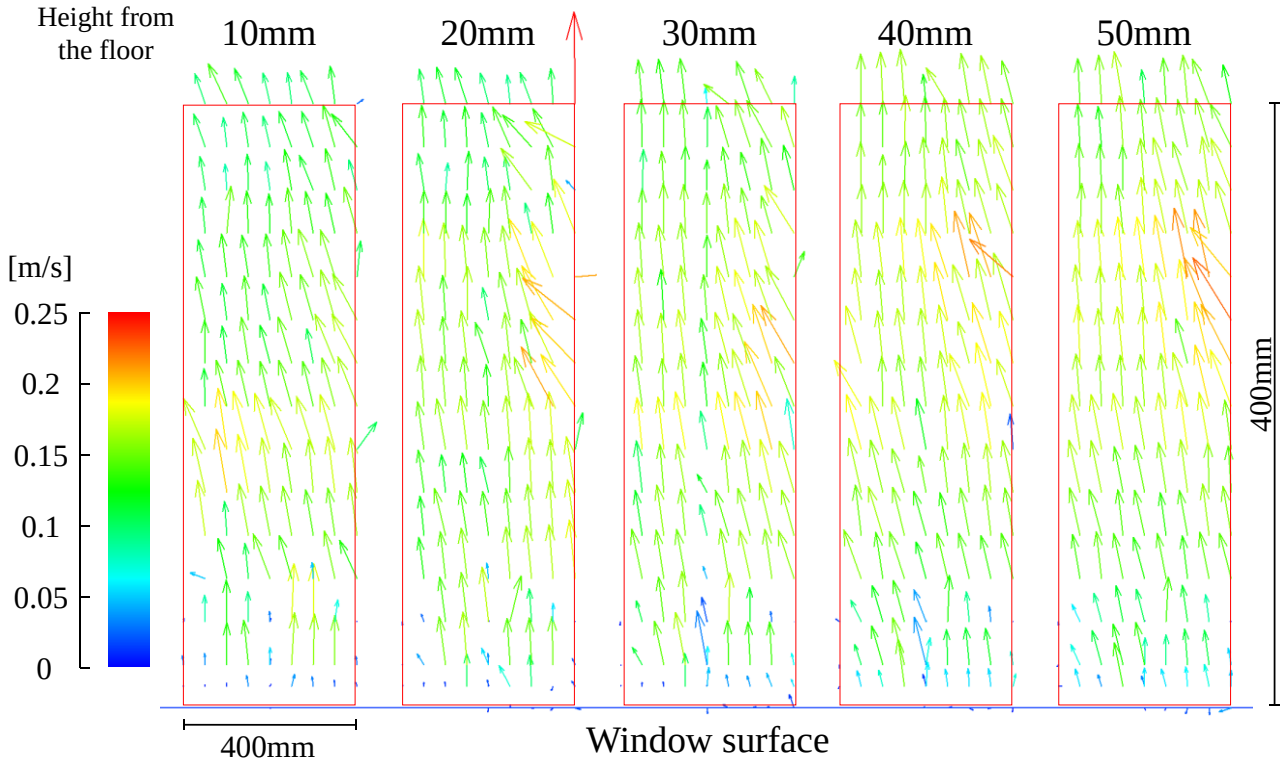


*Figure 8: Experimental results in sections in the XY plane.*

the search-region size increased. However, a large deviation was observed in the mean wind-velocity vector. On the other hand, in contrast, change of the search-region size had almost no influence on the mean wind-speed vector on the left side of the figure where smoke came out clearly.

It was confirmed that the deviation can be more easily determined for increased search-region size. It is necessary to choose suitably by the actual size of the photography territory. Further, 8pixels will be used at the photography reach of the animation used for this verification.

**Removal of an error vector**

For improving analytical accuracy, an error vector was removed when it was below the fixed correlation coefficient used for wind-velocity-data calculation, leaving only good data. The standard correlation coefficient of the removed vector established in this case and its influence upon the mean wind-velocity vector and evaluation time were inspected, as shown in fig. 7. Further, low-correlation-coefficient wind-velocity data was targeted for each frame when removing the error vector. Therefore, as the standard correlation coefficient value increased, it became necessary to pay attention to the evaluation times of the animation becoming ever shorter.

The data that remained consistent with the surrounding coordinates was calculated in the region with long evaluation time in the wind-velocity-vector figure. On the other hand, though evaluating time used the data with the high correlation coefficient at short territory, data scarce in the consistency with the surrounding coordinate is calculated. Even if the correlation coefficient of the remaining data following removal of the error vector exceeded the standard value, the low-evaluation-time region was of low reliability. It is necessary to compare and examine the evaluation-time distribution in every animation. Additionally remove the wind-velocity data in the region where the evaluation time did not meet the fixed standard for analytical accuracy improvement.

## Experimental results

**Experimental techniques**

By this experiment, the reach to 10 mm-50 mm of height of the XY section every 10 mm and the YZ aspect of the X=900mm, a wind-velocity vector was calculated by repeating the experiment 6 times for each velocity and an analysis and equalizing those as shown in fig. 8. The target evaluation time was approximately 90 s. Only an animation including a little range of the evaluating time was equalized after wind-velocity data of the coordinate was removed. Be caused by the reliability of the data is affected by evaluation time. Furthermore, territory was sorted from the XY section window side neighborhood completely, for convenient installation of laboratory instruments.

**XY sections**

The mean wind-speed vector in an XY section is shown in fig. 8. Further, it was difficult that measurement in the window side and the range of the north wall neighborhood takes a picture of a clear animation. Since

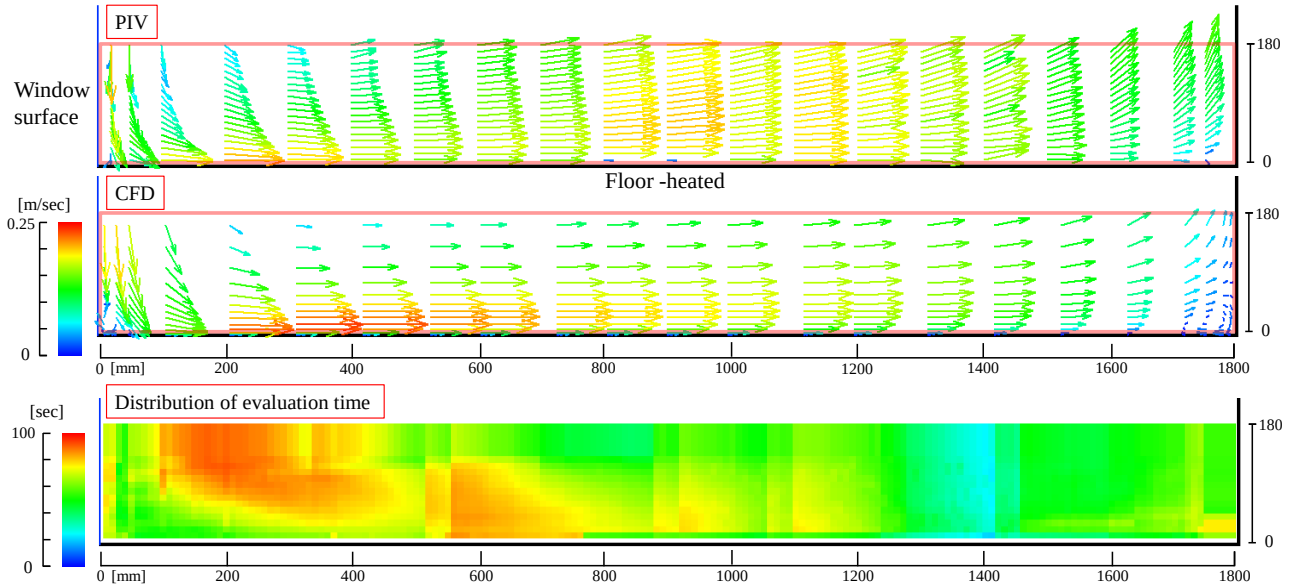


*Figure9: A comparison between CFD analysis and experimental results using PIV in the YZ section.*

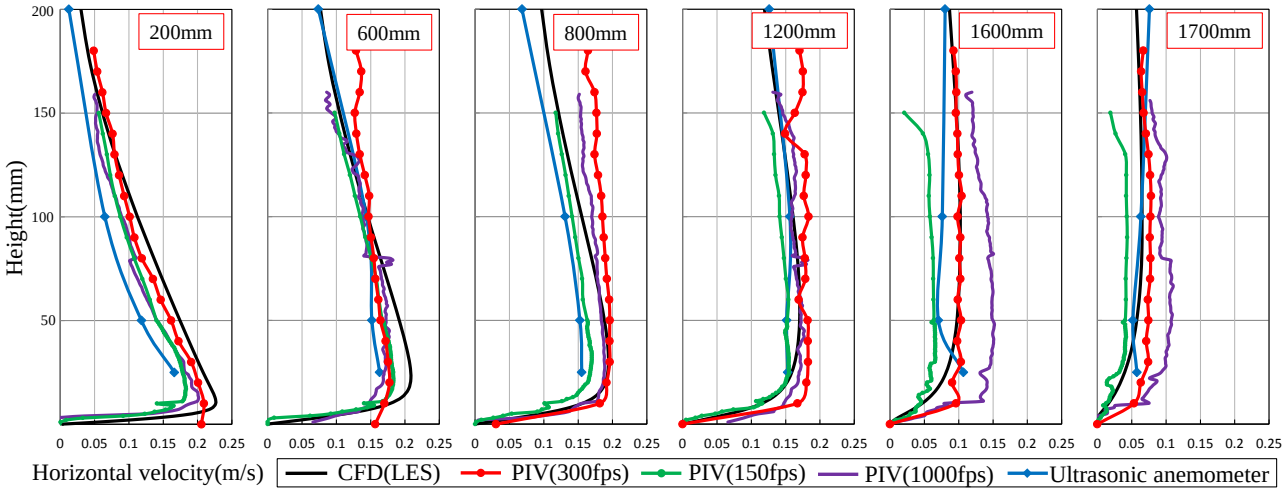


*Figure 10: A comparison of the mean horizontal velocities at different distances from the window.*

the physical relationship was filled with smoke between the high-speed camera and the target seat of measurement. It was the data which can't maintain the consistency with the surrounding territory in particular in the north wall neighborhood. Therefore, only data from the window side up to 1,400 mm was used to create fig. 8.

Around the window side, the wind velocity is at most 0.15 m/s; toward the center of the room, the wind velocity is strengthened to 0.2 m/s at most and the wind velocity ceases to change significantly with height. The wind velocity weakens to 0.1 m/s in the range of heights from 10 to 20 mm with approach to the north wall.

**YZ section**

The mean wind-speed vector and the average time distribution in a YZ section are shown in fig. 9. It depends on cold draft in the window side neighborhood, the wind velocity vector which drops was confirmed. A very weak wind velocity of approximately 0.05 m/s was calculated in the window-side neighborhood of an XY section. On the other hand, it was confirmed that the wind velocity of the verticalness direction is dominant by a coordinate in the window side extreme neighborhood, because the wind velocity of the vertical ingredient was calculated on the window-side extreme neighborhood of a YZ section. The wind velocity in the height range from 10 to 20 mm was strongest approximately 200 mm away from the window side, having a value of 0.2 m/s.

There were no significant differences in the wind-velocity vectors at different heights in the midsection of the electric floor-heating-room model. Further, a wind velocity of approximately 0.15 m/s was determined, stronger than in other regions. The height at which the wind velocity is maximal moves to a higher location than in the window-side neighborhood.

The moderately weak wind velocity near the north wall was calculated, and an ingredient of a vector of looking up increased. The wind velocity about approximately 0.1

m/s was stronger than that in the neighborhood of the floor surface. It was calculated in the height range from 100 to 180 mm.

**Velocity profile**

The wind-velocity profile in the Y-direction was formed using calculated wind-velocity data. Comparisons with previous research results were performed as shown in fig. 10. In the YZ plane comparisons were performed from the resting face to a height of 180 mm at an interval of 10 mm. Also, including the wind-velocity data of the animation which was taken in 150fps and 1000fps.The measured data by Ultrasonic anemometer and by PIV are identical for the most part. Therefore, PIV is practicable as measured data for CFD-code validation.

The slope of the wind velocity was large, and this quantity reached a maximum of 0.2 m/s near the resting face in the vicinity of the window. After that, there is an air current called off to north wall of an electric floor-heating room model by cold draft. This wind velocity near the center of the room tends to be strong. The wind velocity was weakened in the neighborhood of the north wall. Further, the side of this wall was less than 0.1 m/s of the wind velocity from Y = 1,700 mm. As a result of the CFD analysis this tendency chooses as Ono, it's similar.

The change in the wind velocity as a function of height was large in the neighborhood of the south window. While a maximum wind velocity of 0.2 m/s was calculated in the range of 0 to 50 mm from the window side, this tendency weakens toward the center of the room. When approaching the neighborhood of the north wall, a maximum wind velocity of 0.2 m/s was observed between 50 and 150 mm. Further, there was little difference in wind velocity as a function of height. The wind velocity near the floor surface is thought to have been suppressed by friction. Further, the shape of the wind-velocity profile will have the tendency described above.

## Conclusion

Wind-velocity measurement was conducted by using PIV for understanding the natural convective field in a floor-heating-room model and expanding the wind-velocity database for CFD-code validation. It was confirmed that PIV is for the most part capable of measuring the properties of air currents of the natural convective field in the neighborhood of the floor.

## References


Tian, Y.S. and T.G. Karayiannis (2000). Low turbulence natural convection in an air filled square cavity Part I: the thermal and fluid flow fields. *International Journal of Heat and Mass Transfer, 43*, 849–866.

Gandhi, M., Sathe, M., Joshi, J., and P. Vijayan (2011). Two phase natural convection: CFD simulations and PIV measurement. *Chemical Engineering Science*, *66*(14), 3152–3171.

Bangalee, M.Z.I., Miau, J.J., Lin, S.Y., and J.H. Yang (2013). Flow visualization, PIV measurement and CFD calculation for fluid-driven natural cross-ventilation in a scale model. *Energy and Buildings*, *66*, 306–314.

Ono, H., Sakai, K., and T. Kurabuchi (2013). Validation of Accuracy of CFD for Natural Convection Flow in Floor Heating Room. *Proc. of the 7th Int. conference on IAQVEC, PID*

Zhang, X., Su, G., Yu, J., Yao Z., and F. He (2015). PIV measurement and simulation of turbulent thermal free convection over a small heat source in a large enclosed cavity. *Building and Environment, 90*, 105–113.

Ooishi, M., Koji, Sakai (2016). A Study on Grasp of Characteristics Natural Convection Flow in Floor Heating Room, *Architectural Institute of Japan*